A reconfigurable four terminal-pair digitally assisted and fully digital impedance ratio bridge

Jan Kučera, Jakub Kováč

***Abstract*— A reconfigurable digital bridge for calibrations of four terminal-pair defined impedance standards in the whole complex impedance plane by means of fully digital (FD) operation of the bridge and for R-R, C-C calibrations and ac QHR experiments by means of involvement of reference inductive voltage divider (IVD) in digitally assisted (DA) configuration have been built at CMI during last years. For the bridge purposes, a high accuracy digital voltage sources operating in audio frequency range with full isolation between modules and with battery operation mode were developed. Together with coaxial switches with negligible crosstalk between channels, voltage sources form a base for full automation of the calibration process. The bridge was tested in both FD and DA configurations. Depending on the configuration, different relative accuracy of measurements can be achieved in the range from few parts in 10^8 to few parts in 10^5.**

***Index Terms*—audio frequency, automation, impedance bridge, calibration, electric variables measurement, generators, impedance**

I. INTRODUCTION

ELECTRICAL impedance plays a key role in measurements based on evaluation of absolute impedance values or on evaluation of impedance changes in different kinds of devices, such in impedance standards or sensors. Due to increasing demand for calibrations of devices performed in more calibration points (checking of linearity, phase errors, frequency dependence, etc.) in industry, there is a need for automation of calibration processes, together with lowering its uncertainty, provided by national metrology institutes (NMIs). In the case of impedance ratio measurements, there is a need to achieve relative uncertainty level of 10^{-5} in the whole complex plane up to 10^{-8} for in-phase measurements bellow and above kHz frequency range [1]. It was shown, that fully digital bridge can be applied in metrology for calibration of 2-TP (e.g.[2]) or 4-TP defined impedance standards (e.g. [3]). Moreover, a whole calibration chain from QHR to capacitance can be realized by means of FD or DA bridges too [4]. For 1:1 ratio measurements with quantized Hall resistance (QHR), digitally assisted bridge was recently used [5].

This work was partially funded by the EMRP Project SIB53 AIM QuTE, Automated impedance metrology extending the quantum toolbox for electricity. The EMRP is jointly funded by the EMRP participating countries within EURAMET and the European Union.

Jan Kučera is with the Czech Metrology Institute (CMI), 638 00 Brno, Czech Republic (e-mail: jkucera@cmi.cz) and partially with CTU FEE in Prague,.Department of measurements, Prague, Czech Republic.

Jakub Kováč was with the Czech Metrology Institute (CMI), 638 00 Brno, Czech Republic. He is now in cooperation with CMI as an external expert.

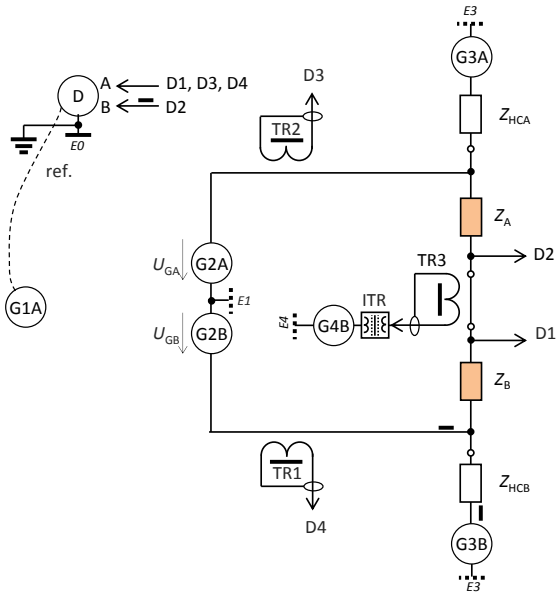

Fig. 1 Principle scheme of fully digital bridge. For simplicity, coaxial wiring is not shown; black rectangles mean current equalizers. Same numbers *i* at points *Ei* denotes grounding points, which are common for paired generator's channels.

New FD and DA bridges together with older manually operated bridges are used in primary impedance laboratories today. It leads to a situation, where the lab has to maintain several measurement setups consisting of different hardware from several suppliers. Other approach is to base all bridges on the same hardware and realize current arms by means of stable generators for both FD and DA bridges instead of auxiliary inductive dividers to achieve full automation of the measurement together with fulfilling four terminal-pair (4-TP, [6]) definition of calibrated standards. Implementation of the reconfigurable FD and DA bridge, described in [7] is given here in details with evaluation of generator's errors.

II. BRIDGE TOPOLOGY

In Fig. 1 is a principle schematic of the fully digital bridge in the configuration for a ratio measurement of two impedances Z_A and Z_B like 4-TP impedances. The reference ratio is formed by means of a two-channel generator with outputs G2A and G2B. The measured ratio of Z_A and Z_B can be derived from:

$$Z_B/Z_A \approx U_{GB}/U_{GA}. \quad (1)$$

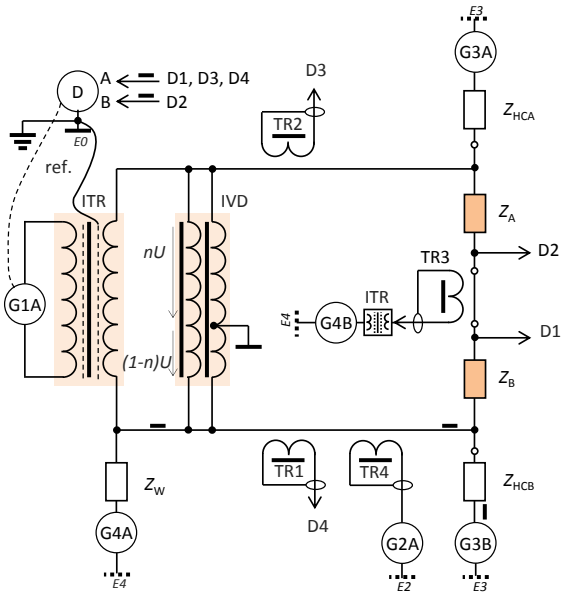

Fig. 2 Principle scheme of digitally assisted bridge.

Fulfilling of 4-TP definition of impedances Z_A, Z_B is maintained by means of current arms formed by G3A and G3B, which are tuned until zero currents flows through high potential arms of Z_A, Z_B. Residual currents are detected by means of voltage measurements at points D3 and D4. An influence of the voltage drop across the current link between Z_A, Z_B is minimized (i.e. voltage difference between points D1 and D2 is negligible) by means of the injection circuit TR3 which is energized from generator G4B via isolation transformer ITR. Finally, 4-TP conditions of compared impedances are fulfilled when voltages detected on the null detector U_{D1}, U_{D3}, U_{D4} and U_{D2}–U_{D1} are equal to zero. Lock-in amplifier with two inputs, which serves as a null detector D, is switched between all measurement points D*i* (*i*=1, .., 4) with a help of a coaxial multiplexer and is synchronized with generators by optically isolated reference signal from generator G1A.

In Fig. 2 is the bridge transformed to DA version, where better accuracy by two or three orders can be achieved by changing reference voltage ratio sources G2A and G2B with an inductive voltage divider IVD with known ratio. The energizing part of this modified bridge consists of the voltage source G1A and an isolation transformer ITR. Voltage source G2A and an injection transformer TR4 serve as the main balance control; from an injected voltage U_{inj} can be evaluated the impedance ratio:

$$Z_B/Z_A \approx (1 - n + U_{inj}/U)/n, \qquad (2)$$

where *n* corresponds to ratio of output and input voltage of the IVD (see Fig. 2). Zero currents in high potential leads of Z_A, Z_B, together with elimination of potential drop on the impedance of the link between Z_A and Z_B are controlled by the same methods like in the case of FD bridge described above. By properly setting Wagner ground circuit formed by Z_W and G4A [8], a no-load condition on the tap of the IVD can be achieved.

III. Bridge Modules

It is clear, that for accuracy of FD bridge is the most critical a knowledge of values of voltages produced by generators G2A and G2B, and an overall stability of all employed generators. For DA bridge, beside conditions which are same for manually operated bridges (described in [8], [9]), is the most critical the accuracy of generator G2A and, again, stability of all employed generators (otherwise fulfilling of all bridge balance conditions in the same time become impossible). Thus, details about developed generators followed by description of other parts are given here.

A. Modular SWG generators

The SWG generator is a modular, battery or power line operated, two channels high accurate voltage source with full isolation between other SWG generators. Principle scheme of one SWG generator module is shown in Fig. 3 [10]. The generator uses Direct Digital Synthesis (DDS) to generate a sine wave signal on the output of each voltage source channel. The DDS is implemented in an FPGA and it consists of a frequency reference, a sine wave look-up table and digital-to-analog converters. The frequency reference can be selected either from an internal clock oscillator (10 MHz) or from an external clock (input ExtCLK) distributed via fiber optics. Using the external clock makes possibility to synchronize multiple generators, which is necessary for the phase shift stability of generated waveforms of multiple generators. The sine wave look-up table of high amplitude and angular resolution is stored in the internal memory. High resolution of the stored sine wave together with a low clock jitter brings the benefit of clean spectrum of the generated signal.

The voltage reference is shared by two voltage sources of the generator module and it can by selected from the internal (intREF) or the external (input ExtREF) 10 V reference. Because the voltage reference is shared by two voltage sources, its time and temperature drift has no influence on the voltage ratio of outputs A and B, which is critical property especially for FD bridges.

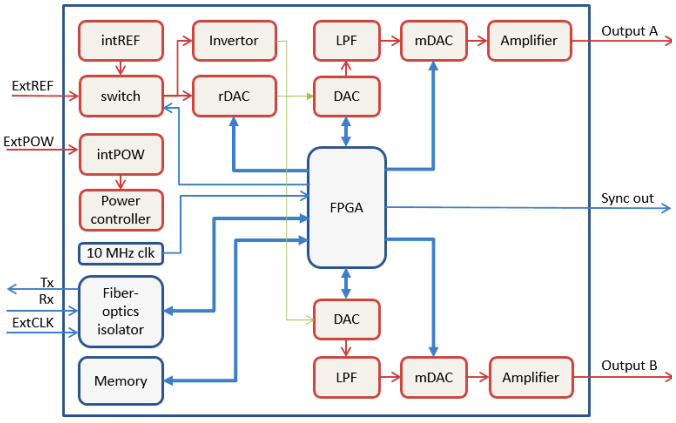

Fig. 3 Principle scheme of the SWG generator.

TABLE I
PROPERTIES OF THE SWG GENERATOR

Quantity	Value
Max. output Voltage (FS)	7 V_{rms}
Amplitude resolution	< 0.01 μV/V of FS
Phase resolution	2×10^{-7} rad
Rel. voltage ratio stability of channels A/B	up to 0.01 $\times10^{-6}$/30 min.
Frequency range at least	10Hz to 20 kHz
SFDR	< -95 dB @ 100 Hz < -85 dB @ 1 kHz
Crosstalk between channels A and B	< -150 dB @ 1 kHz
Reference clock	10 MHz Internal/External
Reference voltage	10 V_{dc} Internal/External

The 20-bits digital-to-analog converter DAC is used to generate a pure sine wave signal with fixed output amplitude. To remove higher harmonics from the output signal, 2nd order low pass filter (LPF) is used after DAC. Output amplitude of the channel is set by 18-bits multiplying circuit mDAC followed by power amplifier. Involvement of mDAC sine wave generation circuit brings an advantage of preserving high SFDR even for small output amplitudes. For getting even higher output resolution than 18-bits, the DAC reference voltage can be adjusted in small range by additional 16-bits circuit rDAC for each channel separately. Then, resolution better than 0.01 μV/V of full scale is achieved.

The SWG generator integrates several protections of the connected devices to prevent them from non-continuous changes of sinewave signal. Any changes of the output amplitude settings and switching on/off channel's output are performed when the signal is crossing zero. Also, the phase shift change of the signal is continuous by a short time frequency sweep. It is useful especially when inductive type of impedance load is connected to the voltage source output. An external device, like lock-in amplifier, can be synchronized by TTL Sync signal, which has the same frequency as the generated signal on A and B outputs.

Fiber optic is used for a communication with the control unit and for the external clock reference input. The SWG generator is powered from an external power supply (extPOW) or from an integrated battery pack (intPOW). Thus, all SWG generator modules can be isolated from each other and crosstalk between them are minimized. Parameter settings are done through a control unit connected to the PC. The control unit has also built in clock reference (with an option for external clock reference), clock distribution network and a battery charger. Properties of SWG generators are summarized in Table I, design of one two-channel module is shown in Fig. 4.

Fig. 4 Design of SWG generator. Voltage output of channel A and B together with center point–ground (left), optic fiber ports for control and external clock (right top), external voltage reference input (right middle), sync out and status LEDs (right bottom). Active air cooling of inner parts improves stability of output voltage under different loads.

B. Coaxial multiplexer

Measurement points D*i* (see Fig. 1 and 2) are during balancing procedure switched to inputs of lock-in amplifier with a help of the coaxial multiplexer. The multiplexer have four independent, fully isolated channels, each consisting of few specially arranged relays and shieldings, ensuring negligible crosstalk between input and output of each opened switching channel (better than -185 dB for signals at 1 kHz [11]). Each channel is controlled independently via an optic fiber. A simplified single switch with shorted output was used as a shorter for IVD output for Wagner ground circuit balancing purposes.

C. Other parts

Injection and detection transformers TR1..4 are designed with ratio100:1, resp. 1:100. When it is necessary to achieve higher ratios in injection circuit of DA bridge, an additional transformer can be added in between TR4 and G2A. The inductive voltage divider is a two-stage type with magnetization winding for lowering errors of main ratio winding and has outputs for 1:1 up to 1:10 voltage ratios. Realization of the bridge is in Fig. 5.

Fig. 5 The FD/DA bridge in DA configuration. Set of four two-channel generators (bottom left), inductive voltage divider lower right, coaxial switches, injection and detection transformers (middle), lock-in amplifier (top), two calculable reference resistance standards (bottom right).

IV. PROPERTIES OF THE BRIDGES

A. *Uncertainty sources*

Uncertainty of impedance ratio measurement with both bridge types depends on residual voltages measured at points D*i* and imperfection of bridge circuits. FD bridge accuracy depends mainly on knowledge of G2A and G2B voltage ratio. Gain error of G2A and G2B can be eliminated by means of performing two measurements with swapping positions of generator's channels A and B in the bridge. Crosstalk between channels has to be evaluated separately. Linearity of generators is due to application of same DACs in all channels usually nearly same, thus any effect of any nonlinearities on ratio measurements cannot be eliminated by same method like their gain error. The linearity can be checked in more steps by means of

a) comparison of ratio U_{GA}/U_{GB} against reference voltage divider with known ratio and phase difference (like an inductive voltage divider with multiple outputs or like known impedance standards),
b) measurement of U_{GA}, U_{GB} with a precision calibrated digitizer,
c) determination of an effect of change of value of multiple bits on the amplitude and the phase error by means of evaluation of voltage difference between U_{GA} and U_{GB}, where DAC or mDAC of G2A is configured like e.g. 00111_b, G2B 00111_b and then G2A is changed to 01000_b. The voltage difference between U_{GA} and U_{GB} is during measurement very small (ideally equal to one LSB step) in comparison with nominal amplitude, so high accuracy of measurement is simply achieved with a lock-in amplifier.

It is necessary to exactly identify any discontinuities in output voltage (differential nonlinearities) and phase of the generators. With method c), with few tens of measurements all discontinuities can be identified. We give here an example of errors identification for 18-bit mDAC, which is performed step by step for each bit *m* of mDAC by means of three measurements for each *m*:

1. a1[1:*m*-1] + a0[*m*:18]
   b1[1:*m*-1] + b0[*m*:18]
2. a1[1:*m*] + a0[*m*+1:18]
   b1[1:*m*-1] + b0[*m*:18]
3. a1[1:*m*] + a0[*m*+1:18]
   b1[1:*m*] + b0[*m*+1:18],

where a1, resp. b1 denotes binary "1" and a0, b0 denotes binary "0" for channels A resp. B. With lock-in amplifier connected between generator's outputs A and B in differential mode, subtraction of second and first measurement corresponds to identification of errors of channel A and subtraction of second and third measurement to identification of errors of channel B. In Fig. 6 are results of in-phase and quadrature errors observed in one mDAC, where errors are

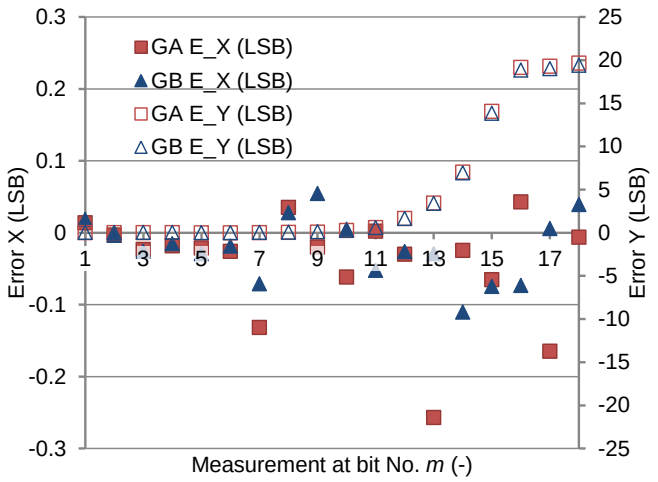

Fig. 6 In-phase (E_X) and quadrature (E_Y) errors introduced in output voltage of generator's outputs A and B, when mDAC is used for modification of output amplitude of the generator and programmed word in mDAC is changed from a1[1:*m*-1]+a0[*m*:18] to a1[1:*m*]+a0[*m*+1:18], resp. b1[1:*m*-1]+b0[*m*:18] to b1[1:*m*]+b0[*m*+1:18]. Measured at frequency 1 kHz.

recalculated from measured voltages to equivalent LSB and corresponds to bit error effects, when values of *m*-1 bits are changed from a1[1:*m*-1] + a0[*m*:18] to a1[1:*m*] + a0[*m*+1:18], resp. b1[1:*m*-1]+b0[*m*:18] to b1[1:*m*] + b0[*m*+1:18]). From measurements of higher *m* one can subtract errors identified for lower *m* in previous measurement steps. Then, observed nonlinearities with appropriate error model of DAC could be used for estimation of amplitude and phase error, alternatively for their corrections. Increase of quadrature error for higher *m* in Fig. 6 does not mean, that at higher *m* is higher phase error, while output amplitude increases too. While only phase errors are significant in our case (see Fig. 7, where quadrature error voltages are expressed in a form of phase error of output

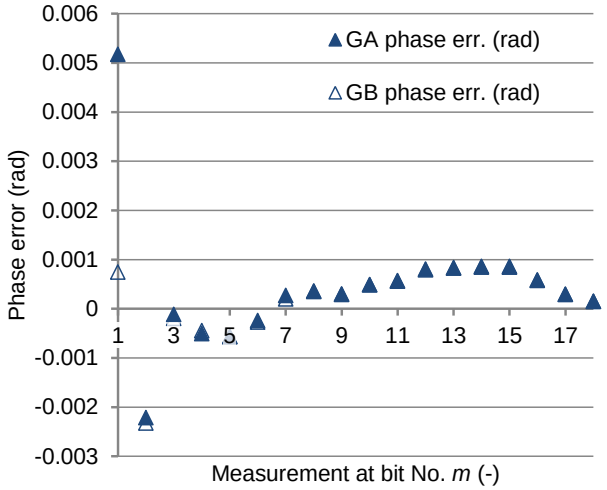

Fig. 7 Equivalent phase errors introduced in output voltage of generator's outputs A and B, when mDAC is used for modification of output amplitude of the generator and programmed word in mDAC is changed from a1[1:*m*-1]+a0[*m*:18] to a1[1:*m*]+a0[*m*+1:18], resp. b1[1:*m*-1]+b0[*m*:18] to b1[1:*m*]+b0[*m*+1:18]. Measured at frequency 1 kHz.

voltage), phase errors has to be carefully taken into account, when FD bridge is used, especially for phase standards calibration.

Uncertainty of FD bridge is influenced by load effects in G2A and G2B too, but due to energizing measurement currents from G3A and G3B, loading currents on G2A and G2B are minimized and consist only of currents flowing through parasitic admittances distributed along generators' outputs and detectors TR1, resp. TR2. In the case of DA bridge, load of IVD instead of G2A and G2B has to be taken into account. Influence of injection circuit consisting of TR4 and G2A (tested by measurement of output voltage of the injection circuit loaded with a dummy load) has to be included too. Moreover, while DA bridge is intended for better accuracy than FD bridge, all appropriate functionality tests of coaxial bridge in accordance with [8] shall be arranged accurately.

Due to used generators, an influence of auxiliary generators' stability on measurement is usually negligible, as can be seen from an example of Allan deviation of the in-phase component of about 10 minutes ratio measurement of NP0 capacitors 500 pF:50 pF (DA bridge configuration) in Fig. 8, where balance on nV level was achieved, which is on the accuracy limits of used lock-in amplifier.

More critical is a stability of resistance of the cabling between Z_A and Z_B low current ports, as can be seen from example measurement of resistance ratio 1 kΩ:100 Ω in Fig. 9. An optimization of contact resistances in cabling between injection transformer TR3 and Z_A, Z_B has to be performed for improvement of resistance measurement stability. In the case of FD bridge, where stability of generators G2A and G2B plays significant role, relative stability on the level 10^{-7} can be achieved, as can be seen from ratio measurement of a phase standard with value -30° (TUBITAK UME) against 1 kΩ in Fig. 10. The Allan deviation is influenced not only bridge components stability, but by measurement frequency near power net higher harmonics too, causing ripples on measured curve.

Overall uncertainty budget for in-phase and quadrature part of measured ratio is evaluated by Monte Carlo method in accordance with [13] and is implemented in NI LabView program. For FD bridge, relative uncertainty for ratio of impedance magnitudes measurement is from level 10^{-7} for R-R or C-C measurements with ratios near 1:1 up to tens of 10^{-5} for ratio 1:15; for DA bridges 10^{-8} up to 10^{-6}, depending on difference between ratio of Z_B/Z_A and IVD. Estimated uncertainty ranges stated above are for frequencies about 1 kHz.

B. Balancing procedure

Bridge balancing procedure implemented in the control program (Fig. 11) is based on secant method [14] and consists of bridge unbalancing followed by iterative bridge balancing. First iteration step is evaluated from an initial bridge state and a programmatically unbalanced bridge state. The unbalancing procedure considers the information from null detector, bridge sensitivity and voltage limits. To achieve balance for all

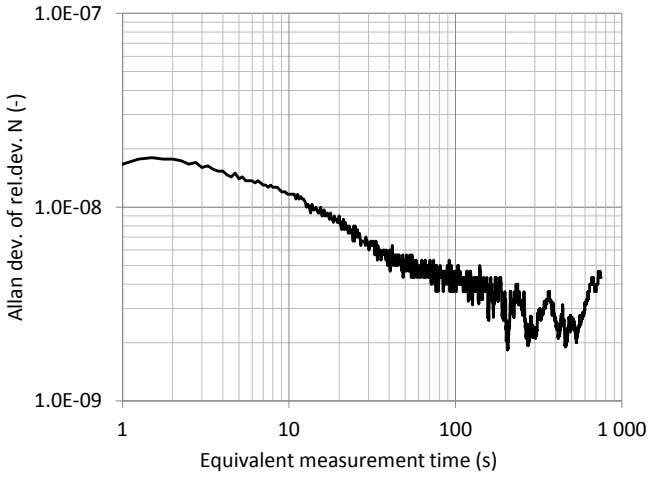

Fig. 8 Allan deviation of the in-phase component of the ratio N=10:-1, measured 500 pF:50 pF @1.59 kHz.

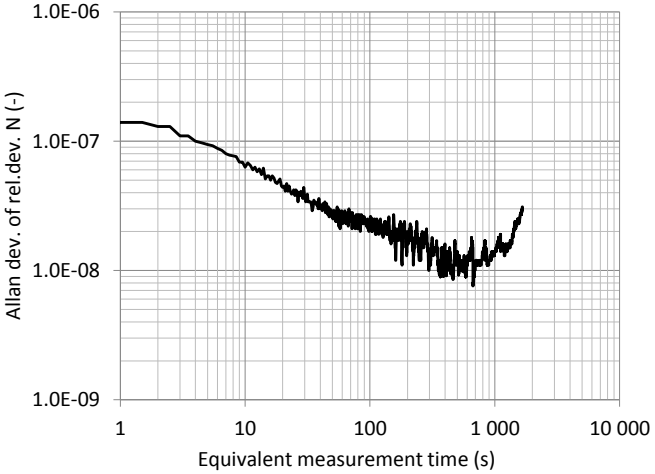

Fig. 9 Allan deviation of the in-phase component of the ratio N=10:-1, measured 1 kΩ:100 Ω @957 Hz.

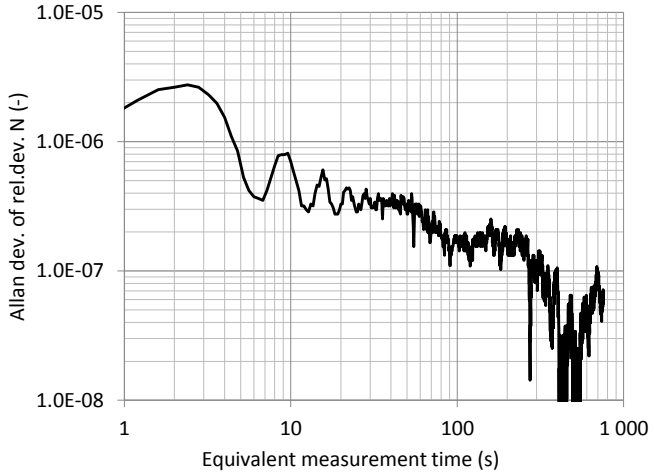

Fig. 10 Allan deviation of the ratio 9.2 kOhm//10 nF:1 kΩ (-30°) @1 000.0003 Hz.

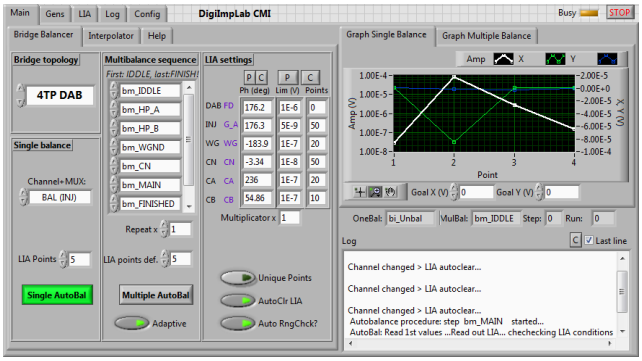

Fig. 11 Program user interface for setting of automated balance conditions. Bridge topology (left), balancing sequence and required accuracy (middle), overview about balancing procedure applied at D_1 (right, in the graph is visible an effect of unbalancing procedure on main balance between measurements No. 1 and 2).

conditions of the bridge, detectors are sequentially connected to a null detector by means of the coaxial multiplexer and the relevant injection is reprogrammed by the control program. The bridge is usually balanced within three iterations of all injection and detector couples within few minutes. An example of successful iteration during balancing the bridge is in Fig. 12.

V. Measurements Results

Series of measurements were performed to verify parameters of developed SWG generators. The SFDR at output frequency 100 Hz and 1 kHz and output amplitude 7.07 Vrms was measured below -95 dB, resp. -85 dB. The one-hour output amplitude stability of one channel was measured below 0.6 µV/V at output amplitude 7.07 Vrms and one-hour output amplitude ratio relative stability of two channels of the single generator module was measured below 0.01×10^{-6}. Phase stability of two channels was better than 0.1 µrad. Two channels crosstalk of the single generator module was measured below -150 dB without load on both channels (which is a typical configuration of G2A and G2B channels in four terminal-pair FD bridge configuration).

Bridges itself were tested with a help of impedance standards with known values. Bellow, results of measurements with

- AH11 type capacitors with nominal values 10 pF and 100 pF (Andeen-Haagerling) and
- resistors with calculable frequency dependence and time constant QFR100 and QFR1000 (with same design like in [15])

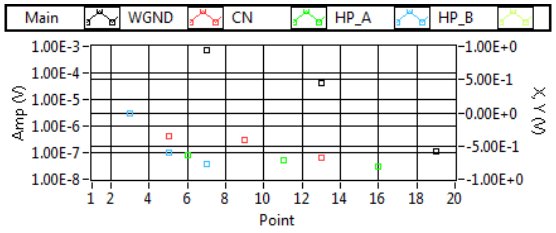

Fig. 12 Workflow of iteration algorithm, where four balances were iteratively balanced (fifth one was within required limits, thus was not balanced again).

are commented. An additional independent verification with capacitors with calculable frequency dependence CXC10 and CXC100 (CTU, [16]) is further planned.

C. FD bridge

For comparison of impedance standards with same nominal values, i.e. for 1:1 ratio measurement was achieved relative accuracy of ratio measurement better than 10^{-6}. More interesting is measurement of different ratios. We performed measurement of 10:1 ratio at frequency 1 kHz, with voltage output of G2A and G2B between 2 % and 100 % of full scale. The results have shown an excellent agreement over wide range of amplitude settings. In Table II are results for resistance and capacitance ratio measurement together with estimated uncertainties (N_{nom} denotes nominal value of the ratio, N_{ref} its calibrated value, N_{FD} ratio obtained from measurement with FD bridge). From results in Table II it seems, that uncertainty budget for measurements with voltages at least between 50 % and 100 % of SWG output full scale is overestimated and could be after further investigation lowered. Ratio N_{ref} of resistance standards was evaluated from DC ratio measurements performed with room temperature current comparator, with additional corrections for their frequency dependence and their drift in time between DC and AC measurements.

D. DA bridge

Most precise evaluation of DA bridge was made by means of resistance standards QFR1000 and QFR100 ratio measurement performed at 1 kHz. Reference ratio was evaluated in similar way like for FD bridge measurements. Due to drifts of QFR standards in time, reference ratio of QFR1000/QFR100 was strongly shifted between measurements with FD and DA bridge. Result of ratio measurement is in Table III. Relative difference between ratios measured with DA bridge N_{DA} and reference value N_{ref} is $+0.023\times10^{-6}$, which is within uncertainty of calculation, resp. measurement (see table IV for uncertainty contributions in the DA bridge measurement). It has to be noted, that such a good agreement was achieved with uncommon high deviation

TABLE II
RATIO MEASUREMENT WITH FD BRIDGE AT 1 KHZ
(UNCERTAINTY CORRESPONDS TO COV. PROB. OF 95%)

Ratio *N*	**Bridge voltage (V_{rms})**	**$N_{ref}/N_{nom}-1$ $\times10^6$**	**$N_{FD}/N_{nom}-1$ $\times10^6$**
QFR 1 kΩ/QFR 100 Ω	1.1	251.5±0.1	260.9±34
AH11 100 pF/AH11 10 pF	7.0	0.3±0.5	-4.1±34
	3.8	0.3±0.5	-2.2±34

TABLE III
RATIO MEASUREMENT WITH AD BRIDGE AT 1 KHZ
(UNCERTAINTY CORRESPONDS TO COV. PROB. OF 95%)

Ratio *N*	Bridge voltage (V_{rms})	$N_{ref}/N_{nom}-1$ $\times10^6$	$N_{DA}/N_{nom}-1$ $\times10^6$
QFR 1 kΩ/QFR 100	1.1	288.583±0.032	288.606±0.039

TABLE IV
CONTRIBUTION OF THE SOURCES OF UNCERTAINTIES FOR QFR 1 kΩ/QFR 100 Ω MEASUREMENT (UNCERTAINTY CORRESPONDS TO COV. PROB. OF 95%)

Quantity *i*	$\mathbf{u_i(N_{DA})}$ $\times\mathbf{10^6}$
IVD calibration	0.009
IVD load	0.012
Current arm Z_A	0.006
Current arm Z_B	0.006
Combining network	0.003
Main balance	0.006
Cable corrections	0.003
Bridge imperfections	0.006
Total	0.039

of the measured ratio from the nominal one.

Important part of the bridge testing is evaluation of quadrature part of the complex impedance ratio too. In Table V are differences of time constants between QFR1000 and QFR100 evaluated from geometrical dimensions of standards and measured by DA, resp. FD bridge. All measurements are in good agreement within uncertainty.

VI. CONCLUSION

A four-terminal-pair FD ratio bridge, easily reconfigurable to DA bridge, has been developed together with precise sinewave generators SWG. Both bridges are based on same equipment. FD and DA configurations were tested by means of comparison of known impedance standards at frequencies near 1 kHz. Results of test measurements were in good agreement with values predicted from geometrical dimensions of standards and reference measurements with other measurement devices. With FD bridge, relative uncertainties of few parts in 10^{-5} and better were achieved. With DA bridge, which is from principle more precise, relative uncertainties of few parts in 10^{-8} were achieved. Investigation of possible errors in DACs involved in generators, which plays major role in overall uncertainty of FD bridge was beside standard error checks focused especially on phase errors caused by differential nonlinearities in DACs. Only few tens of measurements are necessary to identify phase errors of all DAC's bits. Further investigation and modeling is going on.

Beside impedance ratio measurements, DA bridge (with appropriate circuit modifications) is involved in AC measurements of quantum Hall effect for future employment of quantum Hall impedance standard at CMI. Other application of developed DA bridge is calibration of voltage dividers by means of SPCD, which was originally designed for MHz frequencies [17], but it was observed, that after temperature stabilization the SPCD is suitable for high accuracy calibrations at audio frequency range too. FD bridge has been successfully used for comparison of standards with arbitrary phase and impedance values within EMRP Project SIB53 AIM QuTE, where results are under evaluation now.

TABLE V
TIME CONSTANT MEASUREMENTS WITH FD AND DA BRIDGE (UNCERTAINTY CORRESPONDS TO COV. PROB. OF 95%)

Ratio N	τ_{ref} (ns)	τ_{FD} (ns)	τ_{DA} (ns)
QFR 1 kΩ/QFR 100 Ω	-18.3±1.5	-22.0±4.4	-18.7±1.1

ACKNOWLEDGMENT

Authors would like to thank P. Chrobok and L. Vojáčková for reference standards measurements.

REFERENCES

[1] L. Palafox *et al.*, "AIM QuTE: Automated Impedance Metrology extending the Quantum Toolbox for Electricity", 16th International Congress of Metrology, Paris, 11001, 2013.

[2] L. Callegaro, V. D'Elia, M. Kampik, D. B. Kim, M. Ortolano, and F. Pourdanesh, "Experiences With a Two-Terminal-Pair Digital Impedance Bridge," IEEE Trans. On Instr. Meas., 64(6), 2015, pp.1460-1465.

[3] J. Lan, Z. Zhang, Z. Li, Q. He, J. Zhao, and Z. Lu, "A digital compensation bridge for R – C comparisons," Metrologia, 49(3), 2012, pp. 266-272.

[4] L. Callegaro, V. D'Elia, and B. Trinchera, "Realization of the farad from the dc quantum Hall effect with digitally assisted impedance bridges," Metrologia, 47(4), 2010, pp.464-472.

[5] F. Overney, F. Lüönd, and B. Jeanneret, "Broadband fully automated digitally assisted coaxial bridge for high accuracy impedance ratio measurements," Metrologia, 53(3), 2016, pp. 918-926.

[6] R. D. Cutkosky, "Four-terminal-pair networks as precision admittance and impedance standards," IEEE Trans. on Com. and Electron. 83.70, 1964, pp.19-22.

[1] [7] J. Kucera, J. Kovac, "A reconfigurable four terminal-pair digitally assisted and fully digital impedance ratio bridge," IEEE International Instrumentation and Measurement Technology Conference Proceedings (I2MTC 2017)), IEEE, 2017, pp.674-679.

[8] S. Awan, B. P. Kibble and J. Schurr, "Coaxial Electrical Circuits for Interference-Free Measurements," (London U.K.: The Institution of Engineering and Technology), 2011.

[9] L. Callegaro, "Electrical Impedance: Principles, Measurement, and Applications," CRC Press, 2012.

[10] J. Kováč, "Precision low-frequency multichannel generator," diploma thesis, CTU in Prague, FEE, 2014.

[11] J. Kováč, J. Kučera, "A modular coaxial multiplexer with high isolation between channels," XXI IMEKO, Prague, 2015.

[12] J. Kucera, R. Sedlacek, and J. Bohacek, "Improved calculable 4TP coaxial capacitance standards," Digest on Precision Electromagnetic Measurements Conference (CPEM 2014), IEEE, 2014, pp.288-289.

[13] JCGM 102:2011, "Evaluation of measurement data — Supplement 2 to the "Guide to theexpression of uncertainty in measurement" — Extension to any number of output quantities," 2011. [Online: http://www.bipm.org].

[14] L. Callegaro, "On strategies for automatic bridge balancing," IEEE Trans. Instr. Meas., 54(2), 2005, pp. 529-532.

[15] J. Bohacek, J. Kucera, and R. Sedlacek, "Testing calculable resistors of quadrifilar design," Digest on Precision Electromagnetic Measurements Conference (CPEM 2008), 2008, pp.274-275.

[16] J. Kucera, R. Sedlacek and J. Bohacek, "Improved calculable 4TP coaxial capacitance standards," Digest on Precision Electromagnetic Measurements Conference (CPEM 2014), 2014, pp.288-289

[17] J. Kucera, R. Sedlacek and J. Bohacek, "An HF coaxial bridge for measuring impedance ratios up to 1 MHz," Meas. Sci. & Tech., 23(8), 2012, 085004.

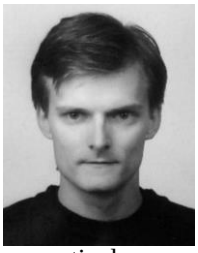

Jan Kučera was born in 1980. He received the M.Sc. degree in measurement and instrumentation and the Ph.D. degree in measurement techniques from the Department of Measurements, Faculty of Electrical Engineering, Czech Technical University in Prague (CTU), Prague, Czech Republic, in 2005 and 2012, respectively.

He joined the Czech Metrology Institute, Prague, in 2011, where he is currently engaged in primary dc resistance and ac impedance metrology. He has been an Assistant Professor with CTU. He has also been involved in research on quantum impedance metrology with Physikalisch-Technische Bundesanstalt, Braunschweig, Germany, since 2008.

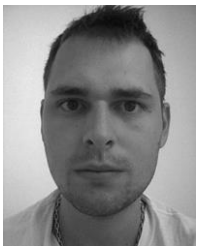

Jakub Kováč was born in Košice, Slovak republic in 1989. He received the B.S. and M.S. degrees in Cybernetics and robotics, field of study Sensors and Instrumentation from the Czech Technical University in Prague (CTU), Prague, Czech Republic.

He was with the Czech Metrology Institute from 2012 to 2014. His research interest was focused on precise measurement of electrical variables and fabrication of precise measurement instruments. Now, he continues his metrology work as an external expert.